Nonlinear Unsharp Masking for Mammogram Enhancement

Karen Panetta, *Fellow, IEEE*, Yicong Zhou, *Member, IEEE*, Sos Agaian, *Senior Member, IEEE*, and Hongwei Jia

***Abstract*—This paper introduces a new unsharp masking (UM) scheme, called nonlinear UM (NLUM), for mammogram enhancement. The NLUM offers users the flexibility 1) to embed different types of filters into the nonlinear filtering operator; 2) to choose different linear or nonlinear operations for the fusion processes that combines the enhanced filtered portion of the mammogram with the original mammogram; and 3) to allow the NLUM parameter selection to be performed manually or by using a quantitative enhancement measure to obtain the optimal enhancement parameters. We also introduce a new enhancement measure approach, called the second-derivative-like measure of enhancement, which is shown to have better performance than other measures in evaluating the visual quality of image enhancement. The comparison and evaluation of enhancement performance demonstrate that the NLUM can improve the disease diagnosis by enhancing the fine details in mammograms with no *a priori* knowledge of the image contents. The human-visual-system-based image decomposition is used for analysis and visualization of mammogram enhancement.**

***Index Terms*—Human-visual-system-based image decomposition, mammogram enhancement, second-derivative-like measure of enhancement (SDME), unsharp masking (UM).**

I. Introduction

BREAST Cancer is the leading cause of death in women between the ages of 35 and 55. The National Cancer Institute estimates that one of the eight women in the United States will develop breast cancer at some point during her lifetime [1]. The mortality rates of 30% in the U.S. and 45% in Europe have been demonstrated by the repeated, randomized, and controlled trials [2]. Currently, there are no effective ways to prevent the breast cancer [3], [4]. However, treatments of breast cancer in the early stages are more successful; therefore, early detection of breast cancer is an important and effective method to significantly reduce the mortality. There are several imaging techniques for breast examination, including MRI, ultrasound imaging, positron emission tomography (PET) imaging, computerized tomography (CT) imaging, optical tomography/spectroscopy, and X-ray imaging. Among them, mammography (X-ray image) is the most common technique for radiologists to detect and diagnose breast cancer [5], [6]. Two types of mammography are currently used: film mammography and digital mammography. Digital mammography is more welcomed by the physicians [7], [8] since it has better image quality, requires a lower X-ray dose [8], has a more confident interpretation for difficult cases, and offers faster diagnosis for routine cases [9].

Due to the limitations of the X-ray hardware systems, screened mammograms even using digital mammography may present low resolution or low contrast, making it difficult to detect tumors at the very early stage. Important indicators of early breast cancer [10], [11], such as irregular-shaped microcalcifications, are very small calcium deposits manifested as granular bright spots in mammograms [12], [13]. The distinction between the tiny malignant tumors and the benign glandular tissue is not readily discernable. Misinterpretation results in unnecessary additional examinations and biopsy [14]. The situation becomes worse when radiologists routinely interpret large numbers of mammograms and can misdiagnose a condition [15].

To improve the visual quality of mammographic images, more image data can be collected at the data acquisition stage, improving the image resolution. However, this significantly increases the overall acquisition time, the amount of radiation that a patient is exposed to, and hardware costs [16]. On the other hand, the image visual quality can be enhanced during the post image processing stage in medical imaging systems. It utilizes different image enhancement techniques to enhance the contrast of mammograms. By this way, the visual quality of mammograms is improved without affecting the acquisition process or increasing the hardware costs.

The underlying concept of mammogram enhancement is to apply image enhancement algorithms to improve the contrast of specific regions or/and objects in mammograms, and then, use a threshold to separate them from their surroundings [11]. To employ it in the medical imaging system, two problems need to be addressed: 1) how to automatically choose the best enhancement algorithm and 2) how to automatically select the thresholding.

Several algorithms for mammogram enhancement have been developed recently. They can be classified into two categories: frequency-domain methods and spatial-domain methods. Here, we give a brief summary on the two categories. More detailed reviews can be found in [11] and [17].

Frequency-domain methods: These methods are based on multiscale representation or fuzzy logic theory. Enhancement

Manuscript received December 8, 2010; revised March 28, 2011 and June 16, 2011; accepted July 31, 2011. Date of publication August 12, 2011; date of current version November 23, 2011. This work was supported in part by the National Science Foundation under Grant HRD-0932339.

K. Panetta is with the Department of Electrical and Computer Engineering, Tufts University, Medford, MA 02155 USA.

Y. Zhou is with the Department of Computer and Information Science, University of Macau, Macau, China (e-mail: yicongzhou@umac.mo).

S. Agaian is with the Department of Electrical and Computer Engineering, University of Texas at San Antonio, San Antonio, TX 78249 USA.

H. Jia is with the First People's Hospital of Pingdingshan, Henan 467000, China.

Color versions of one or more of the figures in this paper are available online at http://ieeexplore.ieee.org.

Digital Object Identifier 10.1109/TITB.2011.2164259

algorithms for mammograms using a multiscale representation first decompose mammograms into a multiscale subband representation using the contourlet transform [18] or different wavelet transforms such as the discrete dyadic wavelet transform [19]–[22], integrated wavelets [23], or redundant discrete wavelet transform [24]. Next, the transform coefficients in each subband of the multiscale representation are modified using different technologies, including nonlinear filtering [25], regression-based extrapolation [26], adaptive unsharp masking (UM) [27], the wavelet shrinkage function [28], or directly contrast modification [29]. Finally, the enhanced mammograms can be obtained from the modified coefficients. However, it has been reported that a wavelet representation does not efficiently show the contours and the geometry of edges in images [18].

Fuzzy set theory has been used to enhance the contrast of mammograms since it is suitable for dealing with the uncertainty associated with the definition of image edges, boundaries, and contrast [4], [30]–[32]. Fuzzy logic has also been successfully integrated with other techniques such as histogram equalization for enhancing medical images [31], and structure tensor for contrast enhancement of microcalcifications in digital mammograms [32].

However, the frequency-domain methods have limitations. They may introduce artifacts called "objectionable blocking effects" [33], or enhance images globally, but not enhance all local details/regions in the image very well. Furthermore, it is very difficult to apply them for automatic image enhancement procedures [34], [35].

Spatial-domain methods: Enhancement algorithms for mammograms in the spatial domain are based on nonlinear filtering [36], [37] and with human visual system (HVS) decomposition [38], adaptive neighborhood [9], [15], [39], [40], or UM [41], [42].

Since nonlinear filtering is known for its ability to obtain more robust characteristics for suppressing noise and preserving edges and details, it is a desirable technique that can be used to enhance mammographic images and other types of medical images. Examples include utilizing the adaptive density-weighted filter [36], the tree-structured nonlinear filters [37], and also adaptive anisotropic filtering [43].

Several other algorithms have been developed for mammogram enhancement using adaptive neighborhood (or region-based) contrast enhancement (ANCE) [9], [15], [39], [40]. The ANCE is intended to improve the contrast of specific regions, objects, and details in mammograms based on local region background and contrast. The region contrast is calculated and enhanced according to the region's contrast, its background, its neighborhood size, and its seed pixel value [9].

UM is another interesting enhancement technique belonging to spatial-domain methods. The traditional UM has good performance to enhance the fine details in the original images. However, it also amplifies noise and overshoots the sharp details at the same time [44], [45]. To overcome this problem, several modification schemes have been developed by replacing the high-pass filter with the adaptive filter [44], quadratic filter [46], and its derived filtering operators called rational UM (RUM) [45] and cubic UM [47]. Other algorithms using UM techniques for mammogram enhancement have been developed [27], [41], [42]. A set of measure metrics for mammogram enhancement is also introduced in [48].

In this paper, we introduce a new nonlinear UM (NLUM) scheme for mammogram enhancement by combining the nonlinear filtering and UM techniques. Leveraging on the advantages of these two techniques, the new scheme can enhance the contrast of specific regions, objects, and details to achieve better visibility of mammographic images for the human observers (radiologists). Furthermore, to address the two questions posed before concerning the automatic selection of the best enhancement algorithm and automatically selecting the threshold, we introduce a new enhancement measure called the second-derivative-like measure of enhancement (SDME). Different parameters in the enhancement algorithm are varied and the results are measured automatically to choose the best on to present. The NULM enhancement performance is demonstrated by the comparison with other existing enhancement algorithms, the quantitative evaluation using the SDME measure, and the receiver operating characteristic (ROC) analysis based on a medical doctor's inspection.

The rest of this paper is organized as follows. Section II reviews several existing enhancement algorithms that are to be compared with the new NLUM scheme, and the operations of the parameterized logarithmic image processing (PLIP) to be consistent with the HVS. Section III introduces the new NLUM scheme. Section IV introduces the new enhancement measure after reviewing several existing ones for quantitatively evaluating the performance of enhancement algorithms. Section V shows the parameter design and optimization for the NLUM scheme using the SDME measure, compares the NLUM scheme with three existing enhancement algorithms, and evaluates the NLUM using the thresholding technique and ROC analysis. Section VI reaches a conclusion.

II. Background

This section briefly discusses traditional UM and four existing enhancement algorithms including RUM [45], ANCE [9], contrast-limited adaptive histogram equalization (CLAHE) [49], and direct image contrast enhancement (DICE) [29]. These algorithms will form the basis for comparison with the new NLUM scheme. The operations of the PLIP are also presented here, and will be used as an operator in the presented NLUM scheme to better represent the HVS response.

A. Traditional UM [46]

The foundation of the traditional UM technique is to subtract a low-pass filtered signal from its original. The same results can be achieved by adding a scaled high-frequency part of the signal to its original. This is equivalent to adding the scaled gradient magnitude back to the original signal. The UM is used to improve the visual quality of images by emphasizing their high-frequency portions that contain fine details as well as noise and sharp details. Therefore, the traditional UM enhances fine details in images and also amplifies noise and overenhances the steep edges at the same time.

B. RUM Algorithm [45]

The RUM uses a rational function operator to replace the high-pass filter in the traditional UM. The rational function is the ratio of two polynomials of the input variables. The RUM is intended to enhance the details in images that contain low and medium sharpness without significantly amplifying noise or affecting the steep edges.

C. ANCE Algorithm [9]

The ANCE was developed to improve the contrast of objects and features with varying size and shape in the mammograms. In this algorithm, each pixel in an image is considered as a seed pixel for a region-growing process. Including the neighborhood pixels whose gray values are within a specified gray-level deviation from the seed, a local region—-called the foreground—is generated around the seed pixel. Another region—called background—consists of those neighborhood pixels that are outside the range of a specified gray-level deviation. The background, which surrounds the foreground, contains nearly the same number of pixels as the foreground. Only regions with low contrast are enhanced, while the high-contrast regions such as steep edges remain unaffected. In order to save computational costs, the redundant pixels in the foreground regions, which have the same values as the seed pixels, are changed to the same new values.

D. CLAHE Algorithm [49]

The normal and adaptive histogram equalizations enhance images using the integration operation. This operation yields large values in the enhanced image for the histogram of the nearly uniform regions of the original image that contains several high peaks. As a result, those enhancement methods may overenhance the noises and sharp regions in the original images. To solve this problem, the CLAHE uses a clip level to limit the local histogram such that the amount of contrast enhancement for each pixel can be limited. This clip level is a maximum value of the local histogram specified by users. An interactive search process is used to redistribute the pixels that are beyond the clip level.

E. DICE Algorithm [29]

The DICE directly amplifies the vertical, horizontal, and diagonal subband components at different levels of the wavelet decomposition, and then, reconstructs them to obtain the enhanced image. The algorithm is used to enhance the mammographic images.

F. PLIP Operations [50]

The PLIP operations use the HVS characteristics that are listed in Table I.

TABLE I
PLIP OPERATIONS

PLIP Operation	Definition
Gray tone function	$g(i,j) = \mu - f(i,j)$
Addition	$g_1 \widetilde{\oplus} g_2 = g_1 + g_2 - \frac{g_1 g_2}{\gamma}$
Subtraction	$g_1 \widetilde{\Theta} g_2 = k\frac{g_1 - g_2}{k - g_2}$
Scalar Multiplication	$c \widetilde{\otimes} g = \gamma - \gamma\left(1 - \frac{g}{\gamma}\right)^c$
Image Multiplication	$g_1 \tilde{*} g_2 = \tilde{\varphi}^{-1}\left(\tilde{\varphi}(g_1)\cdot\tilde{\varphi}(g_2)\right)$ where $\tilde{\varphi}(g) = -\lambda\cdot\ln^{\beta}\left(1-\frac{g}{\lambda}\right)$, $\tilde{\varphi}^{-1}(g) = \lambda\cdot\left(1-\exp\left(\frac{-g}{\lambda}\right)^{1/\beta}\right)$

While $f(i,j)$ is the original image. $g(i,j)$, g, g_1, and g_2 are the gray tone functions to generate negative photos of the original images. $\widetilde{\oplus}, \widetilde{\Theta}$, $\widetilde{\otimes}$ and $\tilde{*}$ are PLIP addition, subtraction, scalar multiplication and image multiplication, respectively. c and β are constants. μ, γ, k and λ are parameters which can be selected as the maximum value of images, or other values. Note that the PLIP addition and scalar multiplication use the same parameter γ because the scalar multiplication is an extension of addition, adding the image to itself c times [50].

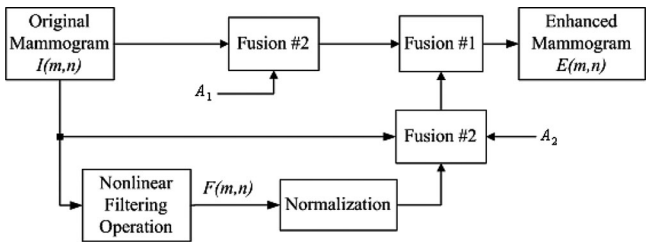

Fig. 1. Block diagram of the new NLUM scheme.

III. NLUM

Integrating the nonlinear filtering operation with UM technique, we introduce a new UM scheme, called NLUM, for mammogram enhancement in this section. This NLUM is a complex UM scheme. It is good at enhancing the fine details of mammographic images.

A. NLUM Scheme

The block diagram of the NLUM scheme is shown in Fig. 1. The original mammogram $I(m,n)$ is filtered by a nonlinear filter. The filtered mammogram $F(m,n)$ is then normalized and combined with the original mammogram using the fusions #1 and #2 to obtain an enhanced mammogram $E(m,n)$.

The nonlinear filtering operation applies a nonlinear operation to the pixels within a 3×3 window. Depending on the different applications, the filtering operation and the fusions #1 and #2 can be selected as the arithmetic operations, the PLIP operations, or nonlinear operations such as the mean square root or logic operations. This property makes the NLUM scheme more general, meeting more complicated requirements for different objects and applications.

If the NLUM scheme uses the arithmetic operations and the fusions #1 and #2 are set to be the arithmetic addition and multiplication, respectively, then the NLUM scheme will resemble

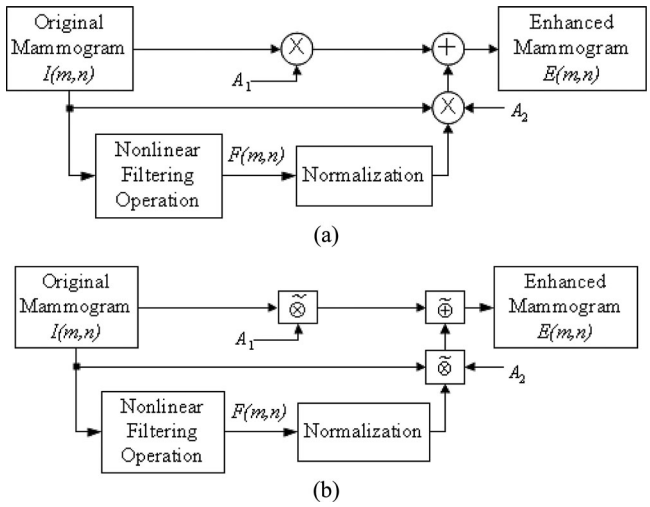

Fig. 2. Practical examples of the NLUM scheme. (a) Using the arithmetic operations. (b) Using the PLIP operations.

the flow, as shown in Fig. 2(a). The enhanced mammogram is defined by

$$E(m,n) = A_1 I(m,n) + A_2 \frac{F(m,n)}{|F|_{\max}} I(m,n) \tag{1}$$

where A_1 and A_2 are the scaling factors and $|F|_{\max}$ is the maximum absolute value of the mammogram, $F(m,n)$, filtered by a 3×3 nonlinear filter defined by

$$F(m,n) = w_0 I_0 + w_1 I_1 + w_2 I_2 \tag{2}$$

where constants w_0, w_1, w_2 are the weight coefficients, and

$$\begin{aligned} I_0 &= I^{2\alpha_0}(m,n) \\ I_1 &= I^{2\alpha_1}(m-1,n) + I^{2\alpha_1}(m+1,n) \\ &\quad + I^{2\alpha_1}(m,n-1) + I^{2\alpha_1}(m,n+1) \\ I_2 &= I^{2\alpha_2}(m-1,n-1) + I^{2\alpha_2}(m+1,n-1) \\ &\quad + I^{2\alpha_2}(m+1,n-1) + I^{2\alpha_2}(m+1,n+1) \end{aligned} \tag{3}$$

where α_0, α_1, and α_2 are the exponential coefficients and $I(\bullet)$is the image pixel intensity value.

On the other hand, if the NLUM chooses the PLIP operations and fusions #1 and #2 are selected as the PLIP addition and multiplication, individually, and then, the NLUM scheme follows the flow, as shown in Fig. 2(b). The NLUM output will change to

$$E(m,n) = A_1 \tilde{\otimes} I(m,n) \tilde{\otimes} A_2 \tilde{\otimes} \left(\frac{F(m,n)}{|F|_{\max}} \tilde{*} I(m,n) \right) \tag{4}$$

where the filtered mammogram $F(m,n)$ is defined as

$$F(m,n) = w_0 \tilde{\otimes} I_0 \tilde{\oplus} w_1 \tilde{\otimes} I_1 \tilde{\oplus} w_2 \tilde{\otimes} I_2 \tag{5}$$

and

$$\begin{aligned} I_0 &= I^{2\alpha_0}(m,n) \\ I_1 &= I^{2\alpha_1}(m-1,n) \tilde{\oplus} I^{2\alpha_1}(m+1,n) \tilde{\oplus} I^{2\alpha_1}(m,n-1) \\ &\quad \tilde{\oplus} I^{2\alpha_1}(m,n+1) \\ I_2 &= I^{2\alpha_2}(m-1,n-1) \tilde{\oplus} I^{2\alpha_2}(m+1,n-1) \\ &\quad \tilde{\oplus} I^{2\alpha_2}(m+1,n-1) \\ &\quad \tilde{\oplus} I^{2\alpha_2}(m+1,n+1) \end{aligned} \tag{6}$$

where $\tilde{\oplus}$, $\tilde{\otimes}$, and $\tilde{*}$ are PLIP addition, scalar multiplication, and image multiplication, respectively; and A_1, A_2, w_0, w_1, w_2, α_0, α_1, and $\alpha_2$are the weight coefficients.

A pseudocode implementation of the NLUM scheme is shown next.

```
Input the original image, I(m,n)
Set values for parameters A1, A2, w0, w1, w2, α0, α1, α2
    Switch (operation)
    Case: linear operation
        if (Fusion #1 = arithmetic addition) && (Fusion #2 = arithmetic multiplication)
            F(m,n) ⇐ apply equation (2) to input image I(m,n)
            E(m,n) ⇐ equation (1)
        end
    Case: PLIP operation
        if (Fusion #1 = PLIP addition) && (Fusion #2 = PLIP multiplication)
            F(m,n) ⇐ apply equation (5) to input image I(m,n)
            E(m,n) ⇐ equation (4)
        end
    end
output the enhanced image, E(m,n)
```

B. Discussion

The NLUM is a complex UM scheme because there are eight coefficients to be specified for practical applications. However, more coefficients offer the NLUM more power and design flexibility to meet more complex and specific requirements in real-world applications.

The nonlinear filtering operation in the NLUM scheme can be designed as a combination of two different types of filters. This offers the NLUM more robust characteristics. For example, the coefficients w_0, w_1, and w_2 can be designed as a high-pass filter and α_0, α_1, and α_2 can be chosen as a center-weighted mean filter.

The users can manually/experimentally select all the NULM coefficients. However, this is a time-consuming method and hard to reach the best enhancement results due to criterion lack for quantitative evaluation. Alternatively, the NULM coefficients could be represented by one or two variables based on some reasonable assumptions to simplify the NLUM design and reduce the number of its coefficients in practical applications. Then, an enhancement measure approach can be used to optimize the coefficients, obtaining the best enhancement result. We will discuss this method experimentally in the Section V-B.

In summary, the presented new NLUM scheme can be an embodiment of the following scenarios:

1) The fusion operators can be defined as different linear or nonlinear operations.
2) The new nonlinear filtering operator can be designed as a combination of different types of filters.
3) The coefficients allow users to change the NULM properties to better meet application-specific requirements.

These scenarios offer the users more design flexibility to adapt the scheme to more specific and complicated requirements in real-world applications. The proposed NULM may also be applied to other imaging modalities.

IV. New Enhancement Measure

Developing a good quantitative measure to assess image enhancement is extremely difficult because the improvement in the enhanced images is often subjective and hard to measure. On the other hand, a good quantitative measure is important for automatically selecting the best enhancement results for computer-aided detection (CAD) systems. In this section, we review several existing methods of measuring the quality of image enhancement, and then, introduce a new enhancement measure using the concept of the second derivative.

A. Existing Enhancement Measures

Several measures of image enhancement have been developed by using a contrast measure. The EME (measure of enhancement) and the EMEE (measure of enhancement by entropy) have been developed by Agaian *et al*. [34]. These two measures are based on a Weber-law-based contrast measure. Later, including the Michelson contrast law, the AME (Michelson law measure of enhancement) and AMEE (Michelson law measure of enhancement by entropy) were introduced to improve the measure performance of the EME and EMEE [35]. Since PLIP subtraction has been shown to be consistent with Weber's contrast law and characteristics of HVS [51], the contrast information can be presented and processed more accurately. Including the PLIP operators to further improve these measures, Panetta *et al*. have developed the logAME (logarithmic Michelson contrast measure) and logAMEE (logarithmic AME by entropy) [52].

All these enhancement measures divide an image into $k_1 \times k_2$ blocks, and then, calculate the average values of the measure results of all blocks in the entire image. The definitions of these measures are listed in Table II.

However, these enhancement measures only calculate the maximum and minimum values of the small regions or blocks in images. As a result, they are sensitive to noise and steep edges in images. To overcome this problem, we introduce a new enhancement measure using the concept of the second derivative since it measures the change ratio of the variation speed of pixel values.

B. New Enhancement Measure

Integrating the idea of the second-derivative-like visibility operator [53] with the strengths of the earlier reviewed measures, we introduce a new enhancement measure called the SDME. It is defined by

TABLE II
Definition of Several Enhancement Measures

Name	Definition
EME	$EME_{k_1k_2} = \frac{1}{k_1k_2}\sum_{l=1}^{k_1}\sum_{k=1}^{k_2}\left[20\ln\left(\frac{I_{\max,k,l}}{I_{\min,k,l}}\right)\right]$
EMEE	$EMEE_{\alpha k_1k_2} = \frac{1}{k_1k_2}\sum_{l=1}^{k_1}\sum_{k=1}^{k_2}\left[\alpha\left(\frac{I_{\max,k,l}}{I_{\min,k,l}}\right)^{\alpha}\ln\left(\frac{I_{\max,k,l}}{I_{\min,k,l}}\right)\right]$
AME	$AME_{k_1k_2} = -\frac{1}{k_1k_2}\sum_{l=1}^{k_1}\sum_{k=1}^{k_2}\left[20\ln\left(\frac{I_{\max,k,l}-I_{\min,k,l}}{I_{\max,k,l}+I_{\min,k,l}}\right)\right]$
AMEE	$AMEE_{\alpha k_1k_2} = -\frac{1}{k_1k_2}\sum_{l=1}^{k_1}\sum_{k=1}^{k_2}\left[\alpha\left(\frac{I_{\max,k,l}-I_{\min,k,l}}{I_{\max,k,l}+I_{\min,k,l}}\right)^{\alpha}\ln\left(\frac{I_{\max,k,l}-I_{\min,k,l}}{I_{\max,k,l}+I_{\min,k,l}}\right)\right]$
logAME	$\log AME_{k_1k_2} = \frac{1}{k_1k_2}\widetilde{\otimes}\sum_{l=1}^{k_1}\sum_{k=1}^{k_2}\left[\frac{1}{20}\widetilde{\otimes}\ln\left(\frac{I_{\max,k,l}\widetilde{\Theta}I_{\min,k,l}}{I_{\max,k,l}\widetilde{\oplus}I_{\min,k,l}}\right)\right]$
logAMEE	$\log AMEE_{k_1k_2} = \frac{1}{k_1k_2}\widetilde{\otimes}\sum_{l=1}^{k_1}\sum_{k=1}^{k_2}\left[\left(\frac{I_{\max,k,l}\widetilde{\Theta}I_{\min,k,l}}{I_{\max,k,l}\widetilde{\oplus}I_{\min,k,l}}\right)\tilde{*}\ln\left(\frac{I_{\max,k,l}\widetilde{\Theta}I_{\min,k,l}}{I_{\max,k,l}\widetilde{\oplus}I_{\min,k,l}}\right)\right]$

Where the image, I, is divided into $k_1 \times k_2$ blocks, α is constant. $I_{\max}$ and $I_{\min}$ are the maximum and minimum of the intensity values in these blocks, respectively.

$$\mathrm{SDME} = -\frac{1}{k_1k_2}\sum_{l=1}^{k_1}\sum_{k=1}^{k_2} 20\ln\left|\frac{I_{\max,k,l}-2I_{\mathrm{center},k,l}+I_{\min,k,l}}{I_{\max,k,l}+2I_{\mathrm{center},k,l}+I_{\min,k,l}}\right| \tag{7}$$

where an image is divided into $k_1 \times k_2$ blocks, $I_{\max,k,l}$ and $I_{\min,k,l}$ are the maximum and minimum values of the pixels in each block separately, and$I_{\mathrm{center},k,l}$ is the intensity of the center pixel in each block. Thus, the size of the blocks should be composed of an odd number of pixels such as 3×3 or 5×5.

Since $I_{\mathrm{center},k,l} \neq \pm 1/2\,(I_{\max,k,l}+I_{\min,k,l})$ according to the SDME definition, the blocks with $I_{\mathrm{center},k,l} = \pm 1/2\,(I_{\max,k,l}+I_{\min,k,l})$ will be discarded while calculating the SDME of an image. Therefore, when $I_{\mathrm{center},k,l}$ approaches $\pm 1/2\,(I_{\max,k,l}+I_{\min,k,l})$, the SDME value will approach infinity; when$I_{\mathrm{center},k,l} = 0$ for all blocks, the minimal SDME value is zero

V. Simulation Results and Evaluations

This section provides the experimental results to discuss the SDME measure performance, the NLUM parameter optimization, the NLUM enhancement analysis, comparison, and evaluation.

A. Comparison of Enhancement Measures

The SDME is compared with six existing measure methods. The measure performance of each method is determined by the consistency of the measure results and subjective evaluation of visual quality of mammograms.

The subjective evaluation method uses the mean opinion score (MOS) recommended by ITU-T [54]. The MOS intends to

TABLE III
SUBJECTIVE EVALUATION FOR THE ENHANCED RESULTS BY DIFFERENT ALGORITHMS

Observer	Original	NLUM	RUM	ANCE	CLAHE
#1	3.5556	4.6111	3.3333	2.6111	1.4444
#2	3.6667	4.9444	3.0000	2.5556	1.7222
#3	3.4444	4.2222	3.1111	2.3889	1.6667
#4	3.7778	4.6889	3.0000	2.3333	2.0000
#5	3.3333	4.8889	3.2222	2.6667	2.6111
#6	3.8889	4.7778	3.2778	2.0000	2.1111
#7	4.1111	4.6667	3.4444	2.4444	1.7778
Average	**3.6825**	**4.6857**	**3.1984**	**2.4286**	**1.9048**

Note: 1 = Bad, 2 = Poor, 3 = Fair, 4 = Good, 5 = Excellent.

TABLE IV
COMPARISON OF MEASURE RESULTS BASED ON DIFFERENT ALGORITHMS

	Original	NLUM	RUM	ANCE	CLAHE
EME	0.9129	1.0833	1.0024	1.0023	2.5425
EMEE	0.0560	0.0688	0.0715	0.0614	0.1961
AME	26.4940	25.1455	26.3165	25.6358	17.4429
AMEE	0.0611	0.0679	0.0619	0.0653	0.1105
logAME	0.0526	0.0485	0.0522	0.0506	0.0316
logAMEE	0.0894	0.0993	0.0894	0.0942	0.1366
SDME	43.6388	47.2091	43.3729	42.2219	35.5386

Note: For each individual enhancement measure, a higher score indicates the better enhancement performance.

determine which are most visually pleasing for a human observer. In this subjective test, seven human observers visually evaluated all original and enhanced mammograms. Each mammogram was given an MOS score of 1–5, where a score of five indicates the best visual quality.

A set of 19 test mammograms is randomly selected from the Internet and the mini-mammographic image analysis society (MIAS) database of mammograms [55]. They are enhanced using four algorithms: the NLUM, RUM, ANCE, and CLAHE algorithms. Therefore, including the original and enhanced mammograms, there are 95 test images in total ($19 \times 5 = 95$) for this comparison. They are evaluated by the subjective method and enhancement measures.

Table III shows the average subjective evaluation scores of each observer for all the test mammograms. The bottom row of Table III shows the average evaluation scores of all human observers on enhanced images categorized by enhancement algorithms. Based on the scores, the NLUM gives the best overall visual quality with a score of 4.6857, while the CLAHE obtains the worst quality with a score of 1.9048.

We then use the SDME and six existing measures to measure the quality of all 95 test images. Each individual enhancement measure has its own data range. A good measure method should yield higher measure results for images with higher visual quality and vice versa.

As shown in Table IV, different measures have diverse evaluation results for these enhancement algorithms. For example, the EME evaluates CLAHE-enhanced images as the best, while the AME gives the highest value to the original images. By comparing the MOS evaluation results in Table III, the SDME is the only measure whose results are consistent with the MOS evaluation results. In the rest of this paper, we use the SDME to assess the enhancement performance of different algorithms.

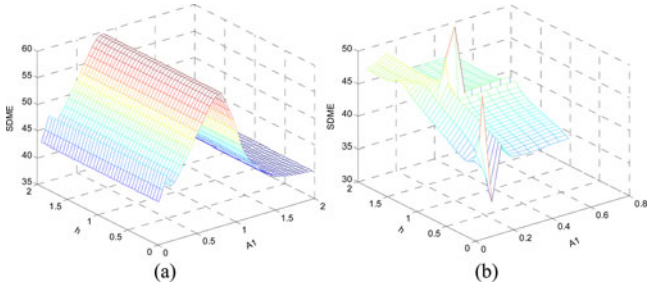

Fig. 3. SDME measure plots of mammogram enhancement based on different A_1 and h. (a) SDME measure graph by arithmetic operation. (b) SDME measure graph by PLIP operation.

B. Parameter Optimization

To demonstrate how to design and automatically optimize the NULM parameters using the presented new SDME, one mammogram obtained from the Internet is used as an example. We then apply the HVS-based image decomposition for the visualization and analysis of the enhanced results. The SDME will also be used to measure and evaluate the performance of the NULM for mammogram enhancement.

To assess the enhancement performance of the presented NLUM scheme, the users have the flexibility to use any existing measure approach for establishing a qualitative metric of mammogram enhancement. The enhancement measure can also be used to optimize all the NLUM coefficients to achieve the best enhanced results. Here, the SDME is selected to measure and evaluate the performance of the NLUM for mammogram enhancement.

There are eight coefficients in the NLUM. To reduce the number of parameters, the user can make assumptions according to the practical design requirements. For example, 1) $A_2 = 1/A_1$, $w_0 = 2$, $\alpha_0 = 8h$, $\alpha_1 = \alpha_2 = h$, and $w_1 = w_2 = -0.125$; or 2)$A_2 = 20A_1$, $w_0 = 8h$, $\alpha_0 = 12h$, $\alpha_1 = h$, $\alpha_2 = 2h$, and $w_1 = w_2 = -h$. These assumptions design the nonlinear filter as a combination of a high-pass filter (w_0, w_1, w_2) and a low-pass filter $(\alpha_0, \alpha_1, \alpha_2)$. More weight is given to the filtered image in order to enhance the fine details in images.

With aforementioned assumptions, all the NULM coefficients are correlated with the parameters A_1 and h. Here, we select the assumption 1) to show how to automatically design the NULM.

By automatically changing the parameters A_1 and h, several enhanced mammograms are generated, and then, measured by the SDME. The measure results are plotted as a graph. The parameters giving the best enhanced result can be located at the points where the SDME curve reaches the local extrema.

Different fusion operations can be used in the NLUM scheme. Here, we compare the arithmetic operation with the PLIP version. Taking Fig. 4(a) as a test image, the SDME measure results of the enhanced mammograms by the NLUM with arithmetic and PLIP operations are plotted in Fig. 3. From measure results, we can find the location of parameters A_1 and h that yield the best enhanced result for each operation.

By using the parameters obtained from the measure in Fig. 3, the original mammogram is enhanced by the presented NLUM with the arithmetic and PLIP operations, respectively. The

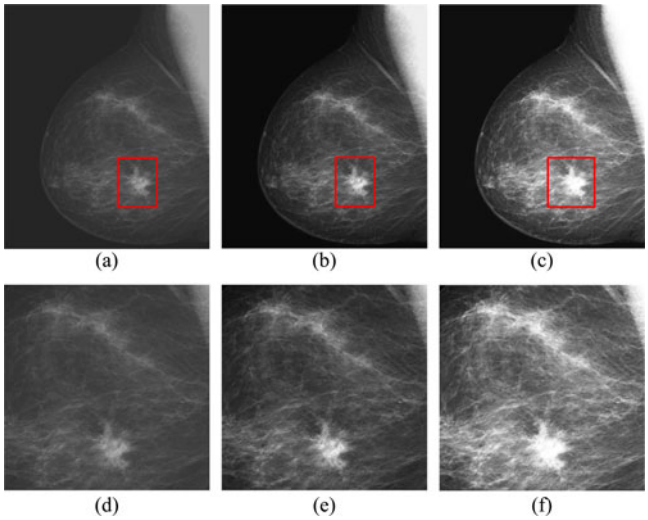

Fig. 4. Mammogram enhancement. (a) Original mammogram. (b) Enhanced mammogram by the NLUM with arithmetic operation. (c) Enhanced mammogram by the NLUM with PLIP operation. (d) Cropped region of (a). (e) Cropped region of (b). (f) Cropped region of (c).

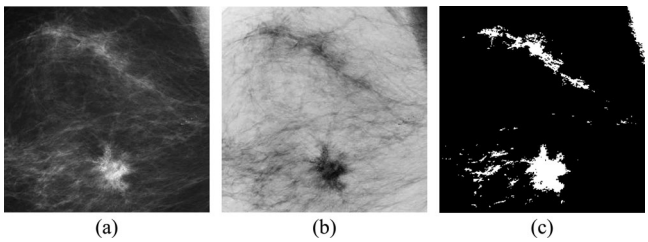

Fig. 5. Enhancement analysis. (a) Enhanced Region cropped form the mammogram in Fig. 4(b). (b) Negative photograph of (a). (c) Thresholding of (a).

enhanced mammograms and their cropped abnormal regions are shown in Fig. 4. The visual quality and local contrast of the enhanced mammograms are much better than that of the original one. The fine details such as microcalcifications and masses in the original mammogram are significantly improved. The abnormal regions are more recognizable in the enhanced mammograms.

Compared with the enhanced results obtained by using two types of fusion operations in Fig. 4, the arithmetic operation shows better performance because the NLUM based on PLIP operation slightly overenhances the mass region, as shown in Fig. 4(c). Therefore, we choose the arithmetic operation for the NLUM to enhance the mammograms in the rest of this paper.

C. Enhancement Analysis

There are many different methods to analyze the enhanced images. Fig. 5 provides two examples: the negative view and thresholding of the specific region of interest (ROI). The shape of the abnormal regions is very clear and easily discernable. This demonstrates the NULM excellent performance for improving the contrast of specific regions, objects, and details in mammograms.

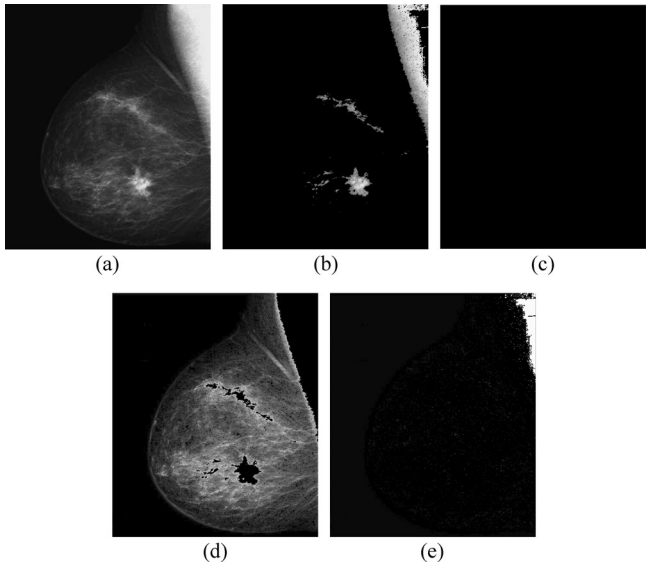

Fig. 6. HVS-based decomposition of the enhanced mammogram. (a) Enhanced mammogram. (b) First subimage. (c) Second subimage. (d) Third subimage. (e) Fourth subimage.

D. HVS-Based Analysis and Visualization

While the user can view the entire image's enhanced results, the process would be improved if only the abnormalities could be emphasized during analysis. Instead of using the segmentation algorithms, the HVS-based decomposition can be used as an alternative method to provide the visualization of results that isolate ROIs, mainly the abnormalities.

By using the background intensity and the rate of information change, HVS-based decomposition separates images into four subimages based on four defined regions: 1) region 1: the saturation region for overilluminated areas; 2) region 2: the Weber region for properly illuminated areas; 3) region 3: the Devries–Rose region for underilluminated areas; and 4) region 4: the fourth region for all pixels containing the least informative pixels [56], [57]. We extend its application to enhancement analysis and visualization.

Figs. 6 and 7 show the HVS-based decomposition results of the enhanced mammogram and its negative (tonal inversion), respectively. In general, the mass regions can be segmented by HVS-based decomposition in one subimage without any segmentation algorithm involved. The results are shown in Figs. 6(b) and 7(d). Therefore, HVS-based decomposition can be used for segmentation and classification of pathological cases in a CAD system.

E. Comparison of Enhancement Performance

In this section, after demonstrating how to automatically optimize the parameters in NLUM, we will apply it to more mammograms and compare it with other well-known enhancement algorithms.

The mammograms for this comparison are obtained from the mini-MIAS database of mammograms [55]. The database consists of 322 mammograms. The cases of patient records range

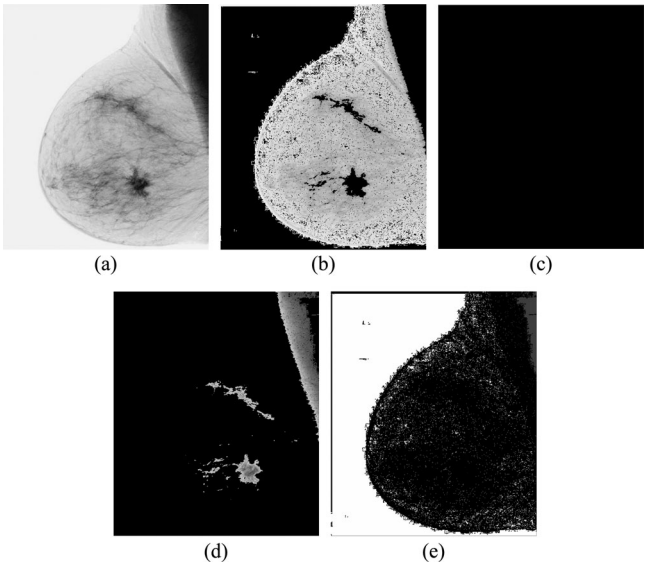

Fig. 7. HVS-based decomposition of the inversed mammogram. (a) Negative of the image of the enhanced mammogram. (b) First subimage. (c) Second subimage. (d) Third subimage. (e) Fourth subimage.

from fairly dense to extraordinarily dense breast parenchyma. Some cases are completely fatty. Most masses have ill-defined, indistinct, or speculated.

All test mammograms are cropped into images with smaller sizes for analysis such that the resulting cropped mammographic images contain most of microcalcifications, masses and abnormal regions that may be interesting to radiologists. These mammograms have limited black background that contains nonobject regions and background project noise.

Six mammograms are used as examples and the enhanced results are shown in Figs. 8 and 9. They clearly show how the enhancement algorithms change fine details and abnormal regions in images. Their SDME results are shown in Table V.

The RUM slightly improves the visual quality of images, but it generates spot artifacts, as shown in Figs. 8(c) and 9(c). The ANCE has very limited visual improvement and produces many textile artifacts for the mammograms. The CLAHE overenhances the background of all mammograms, making microcalcifications and/or mass more unrecognizable than the original ones. As evident from Figs. 8(f) and 9(f), the DICE improves the contrast of the microcalcifications, but it fails to enhance mass regions. It also generates background noise and textile artifacts.

The measure results in Table V demonstrate this. The presented NLUM outperforms the others since it improves the contrast of mammograms and visual quality of the abnormal regions such as mass and/or microcalcifications. The enhanced mammograms have no detail information loss. These are useful for detecting and diagnosing diseases or breast cancer at the early stage. The measure results in Table V verify the NULM excellent enhancement performance.

F. ROC Evaluation

The ROC or the ROC curve is originally developed in signal detection theory. It is a well-known evaluation methodology

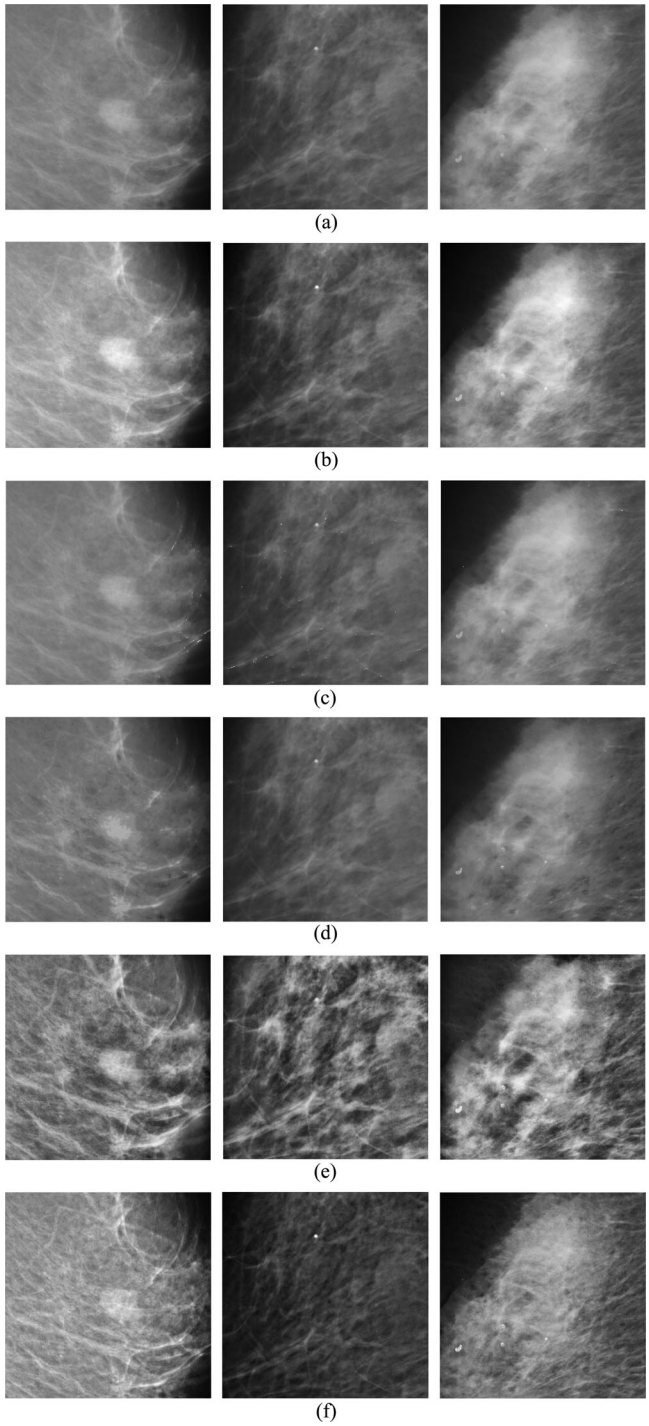

Fig. 8. Comparison of mammogram enhancement using different algorithms. (a) Original mammograms: Mam_1 to Mam_3. (b) Enhanced results by the NLUM. (c) Enhanced results by the RUM. (d) Enhanced results by the ANCE. (e) Enhanced results by the CLAHE. (f) Enhanced results by the DICE.

used for medical decision-making and medical diagnostic imaging systems [58], [59]. The ROC curve is a graphical plot of the true positive rate (a fraction of true positives over the positives) versus the false positive rate (a fraction of false positives over the negatives). To determine whether a person has a specific disease in the clinic diagnosis, a true positive case occurs when the person tests positive and actually has the disease. A false

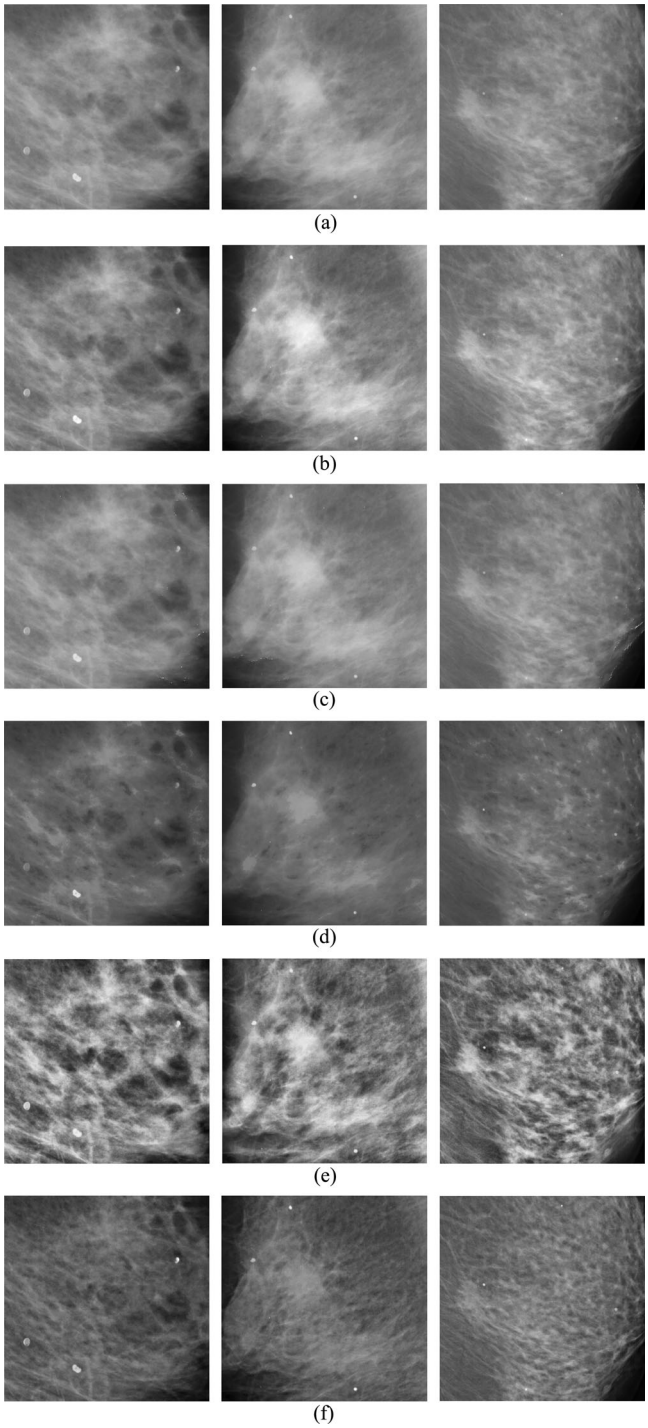

Fig. 9. Comparison of mammogram enhancement using different algorithms. (a) Original mammograms: Mam_4 to Mam_6. (b) Enhanced results by the NLUM. (c) Enhanced results by the RUM. (d) Enhanced results by the ANCE. (e) Enhanced results by the CLAHE. (f) Enhanced results by the DICE.

positive case, on the other hand, occurs when the person tests positive but actually does not has the disease [60]. The MATLAB implementation of the ROC analysis is addressed in [61] and [62].

This section uses the ROC curve to evaluate the NULM enhancement performance. A total of 60 mammograms were selected from the mini-MIAS database. They consist of 30 normal mammograms (which do not contain suspect regions such as calcifications and masses) and 30 abnormal mammograms. All mammograms were cropped into images with smaller sizes such that the resulting images have minimal background or contain most of abnormal regions such as microcalcifications and masses.

TABLE V
SDME RESULTS OF ENHANCED MAMMOGRAMS BY DIFFERENT ALGORITHMS

	Original	NLUM	RUM	ANCE	CLAHE	DICE
Mam_1	44.7378	47.4100	44.5905	41.9886	36.1296	39.748
Mam_2	42.4422	44.7627	42.1725	42.4422	34.2108	37.12654
Mam_3	44.1716	46.9127	44.1132	42.0401	35.8518	39.03196
Mam_4	45.3980	47.6609	45.2934	42.0689	36.2382	39.94165
Mam_5	46.7206	49.7931	46.6719	44.6588	37.5773	41.72588
Mam_6	45.0838	47.6866	44.9040	42.1152	35.9426	39.9139

Note: A higher score indicates the better enhancement performance.

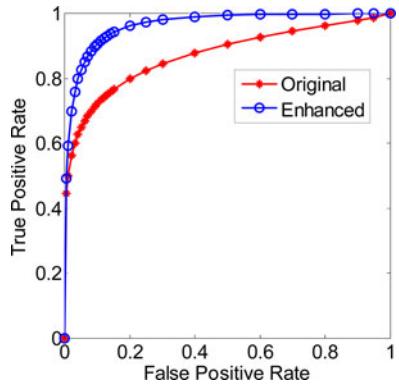

Fig. 10. ROC curves of the original and enhanced test mammograms.

All mammograms were enhanced by the NLUM, and then, divided in two groups: the original and enhanced mammograms. They were inspected by the coauthor, a medical doctor who has a long-term clinic experience of viewing mammograms. The doctor marked each mammogram with the case type ("0" for the truly negative case indicating a completely normal mammogram and "1" for the truly positive case referring to an abnormal mammogram.) and the confidence rate for each case type. The confidence rate is from 1 to 5, where "1" indicates a definitely negative case and "5" means definitely positive [62].

By using an online code of the ROC analysis developed by Eng [62], the doctor's inspection results were plotted into ROC curves for the original and enhanced mammograms, individually. The results are shown in Fig. 10.

The area under the ROC curve (AUC) is used to quantitatively evaluate the classification performance of the diagnosis system [58], [59]. The AUC value is always between 0 and 1. A higher AUC value indicates a better classification performance. The AUC for the enhanced mammogram is 0.957, while the AUC for the original ones is 0.874. This demonstrates that the NLUM enhancement improves the doctor's diagnosis. It has potential use for the improvement of breast cancer diagnosis and detection in the CAD systems.

VI. CONCLUSION

This paper has introduced a new NLUM scheme for mammogram enhancement. The NLUM has been shown to provide more

design flexibility that makes it possible to meet more specific and complex requirements in real-world applications. The simulation results have demonstrated that the NULM parameters can be optimized by the enhancement measure to obtain the better enhanced result for clinical applications. Enhancement comparison has proven that the NLUM shows better performance for improving the local contrast of specific regions and fine details in mammograms. The NLUM has potential applications for improving the automatic disease detection and diagnosis in CAD systems.

To quantitatively evaluate the NULM performance for mammogram enhancement, we have introduced a new enhancement measure called the SDME. Compared with other existing measure methods, the SDME shows better performance for enhancement measure and assessment. The HVS-based decomposition has been verified to be a useful tool to analyze and display abnormal regions in mammograms.

ACKNOWLEDGMENT

The authors like to thank Dr. G. Ramponi at University of Trieste, Trieste, Italy, for providing the MATLAB code for the rational UM algorithm in [45] and his valued consultation. They thank Dr. R. M. Rangayyan and Dr. L. Shen at the University of Calgary, Alberta, Canada, for providing the C code for the ANCE algorithm in [9] and their valued discussion. They also thank the anonymous reviewers for their valued comments that helped to improve the manuscript.

REFERENCES

[1] L.-M. Wun, R. M. Merrill, and E. J. Feuer, "Estimating lifetime and age-conditional probabilities of developing cancer," *Lifetime Data Anal.*, vol. 4, pp. 169–186, 1998.

[2] D. B. Kopans, "The 2009 U.S. preventive services task force guidelines ignore important scientific evidence and should be revised or withdrawn," *Radiology*, vol. 256, pp. 15–20, 2010.

[3] D. E. Stewart, A. M. Cheung, S. Duff, F. Wong, M. McQuestion, T. Cheng, L. Purdy, and T. Bunston, "Attributions of cause and recurrence in long-term breast cancer survivors," *Psycho-Oncology*, vol. 10, pp. 179–183, 2001.

[4] H. D. Cheng and H. Xu, "A novel fuzzy logic approach to mammogram contrast enhancement," *Inf. Sci.*, vol. 148, pp. 167–184, 2002.

[5] R. Mousa, Q. Munib, and A. Moussa, "Breast cancer diagnosis system based on wavelet analysis and fuzzy-neural," *Expert Syst. Appl.*, vol. 28, pp. 713–723, 2005.

[6] X. Gao, Y. Wang, X. Li, and D. Tao, "On combining morphological component analysis and concentric morphology model for mammographic mass detection," *IEEE Trans. Inf. Technol. Biomed.*, vol. 14, no. 2, pp. 266–273, Mar. 2010.

[7] R. A. Smith, V. Cokkinides, and H. J. Eyre, "American cancer society guidelines for the early detection of cancer,," *CA Cancer J. Clin.*, vol. 56, pp. 11–25, Jan. 2006.

[8] S. A. Feig and M. J. Yaffe, "Digital mammography," *Radiographics*, vol. 18, pp. 893–901, Jul. 1998.

[9] W. M. Morrow, R. B. Paranjape, R. M. Rangayyan, and J. E. L. Desautels, "Region-based contrast enhancement of mammograms," *IEEE Trans. Med. Imag.*, vol. 11, no. 3, pp. 392–406, Sep. 1992.

[10] L. Wei, Y. Yang, M. N. Wernick, and R. M. Nishikawa, "Learning of perceptual similarity from expert readers for mammogram retrieval," *IEEE J. Sel. Topics Signal Proces.*, vol. 3, no. 1, pp. 53–61, Feb. 2009.

[11] J. Tang, R. M. Rangayyan, J. Xu, I. E. Naqa, and Y. Yang, "Computer-aided detection and diagnosis of breast cancer with mammography: Recent advances," *IEEE Trans. Inf. Technol. Biomed.*, vol. 13, no. 2, pp. 236–251, Mar. 2009.

[12] H. Li, K. J. R. Liu, and S. C. B. Lo, "Fractal modeling and segmentation for the enhancement of microcalcifications in digital mammograms," *IEEE Trans. Med. Imag.*, vol. 16, no. 6, pp. 785–798, Dec. 1997.

[13] S. Halkiotis, T. Botsis, and M. Rangoussi, "Automatic detection of clustered microcalcifications in digital mammograms using mathematical morphology and neural networks," *Signal Process*, vol. 87, pp. 1559–1568, 2007.

[14] S. Timp, C. Varela, and N. Karssemeijer, "Computer-aided diagnosis with temporal analysis to improve radiologists' interpretation of mammographic mass lesions," *IEEE Trans. Inf. Technol. Biomed.*, vol. 14, no. 3, pp. 803–808, May 2010.

[15] R. M. Rangayyan, L. Shen, Y. Shen, J. E. L. Desautels, H. Bryant, T. J. Terry, N. Horeczko, and M. S. Rose, "Improvement of sensitivity of breast cancer diagnosis with adaptive neighborhood contrast enhancement of mammograms," *IEEE Trans. Inf. Technol. Biomed.*, vol. 1, no. 3, pp. 161–170, Sep. 1997.

[16] I. Larrabide, A. A. Novotny, R. A. Feijóo, and E. Taroco, "A medical image enhancement algorithm based on topological derivative and anisotropic diffusion," peresented at the 26th Iberian Latin-American Congress on Computational Methods in Engineering, Guarapari, Espírito Santo, Brazil, 2005.

[17] A. Papadopoulos, D. I. Fotiadis, and L. Costaridou, "Improvement of microcalcification cluster detection in mammography utilizing image enhancement techniques," *Comput. Biol. Med.*, vol. 38, pp. 1045–1055, 2008.

[18] Z. Lu, T. Jiang, G. Hu, and X. Wang, "Contourlet based mammographic image enhancement," in *Proc. 5th Int. Conf. Photon. Imag. Biol. Med.*, 2007, pp. 65340M-1–65340M-8.

[19] A. Laine, F. Jian, and Y. Wuhai, "Wavelets for contrast enhancement of digital mammography," *IEEE Eng. Med. Biol. Mag.*, vol. 14, no. 5, pp. 536–550, Sep./Oct. 1995.

[20] A. F. Laine, S. Schuler, F. Jian, and W. Huda, "Mammographic feature enhancement by multiscale analysis," *IEEE Trans. Med. Imag.*, vol. 13, no. 4, pp. 725–740, Dec. 1994.

[21] A. Mencattini, M. Salmeri, R. Lojacono, M. Frigerio, and F. Caselli, "Mammographic images enhancement and denoising for breast cancer detection using dyadic wavelet processing," *IEEE Trans. Instrum. Meas.*, vol. 57, no. 7, pp. 1422–1430, Jul. 2008.

[22] P. Sakellaropoulos, L. Costaridou, and G. Panayiotakis, "A wavelet-based spatially adaptive method for mammographic contrast enhancement," *Phys. Med. Biol.*, vol. 48, pp. 787–803, 2003.

[23] P. Heinlein, J. Drexl, and W. Schneider, "Integrated wavelets for enhancement of microcalcifications in digital mammography," *IEEE Trans. Med. Imag.*, vol. 22, no. 3, pp. 402–413, Mar. 2003.

[24] S. Skiadopoulos, A. Karahaliou, F. Sakellaropoulos, G. Panayiotakis, and L. Costaridou, "Breast component adaptive wavelet enhancement for soft-copy display of mammograms," in *Proc. Int. Workshop Digital Mammography*, 2006, pp. 549–556.

[25] C.-M. Chang and A. Laine, "Coherence of multiscale features for enhancement of digital mammograms," *IEEE Trans. Inf. Technol. Biomed.*, vol. 3, no. 1, pp. 32–46, Mar. 1999.

[26] G. Derado, F. DuBois Bowman, R. Patel, M. Newell, and B. Vidakovic, "Wavelet Image Interpolation (WII): A wavelet-based approach to enhancement of digital mammography images," in *Proc. Int. Symp. Bioinformat. Res. Appl.*, 2007, pp. 203–214.

[27] F. Y. M. Lure, P. W. Jones, and R. S. Gaborski, "Multiresolution unsharp masking technique for mammogram image enhancement," in *Proc. SPIE Med. Imag.*, Newport Beach, CA, 1996, pp. 830–839.

[28] J. Scharcanski and C. R. Jung, "Denoising and enhancing digital mammographic images for visual screening," *Comput. Med. Imag. Graph.*, vol. 30, pp. 243–254, 2006.

[29] J. Tang, X. Liu, and Q. Sun, "A direct image contrast enhancement algorithm in the wavelet domain for screening mammograms," *IEEE J. Sel. Topics Signal Process.*, vol. 3, no. 1, pp. 74–80, Feb. 2009.

[30] F. Sahba and A. Venetsanopoulos, "Contrast enhancement of mammography images using a fuzzy approach," in *Proc. 2008 30th IEEE Annu. Int. Conf. Eng. Med. Biol. Soc.*, pp. 2201–2204.

[31] I. Stephanakis, G. Anastassopoulos, A. Karayiannakis, and C. Simopoulos, "Enhancement of medical images using a fuzzy model for segment dependent local equalization," in *Proc. 2003 3rd Int. Sym. Image Signal Process. Anal.*, vol. 2, pp. 970–975.

[32] J. Jiang, B. Yao, and A. M. Wason, "Integration of fuzzy logic and structure tensor towards mammogram contrast enhancement," *Comput. Med. Imag. Graph.*, vol. 29, pp. 83–90, 2005.

[33] S. Aghagolzadeh and O. K. Ersoy, "Transform image enhancement," *Opt. Eng.*, vol. 31, pp. 614–626, 1992.

[34] S. S. Agaian, K. Panetta, and A. M. Grigoryan, "Transform-based image enhancement algorithms with performance measure," *IEEE Trans. Image Process.*, vol. 10, no. 3, pp. 367–382, Mar. 2001.
[35] S. S. Agaian, B. Silver, and K. A. Panetta, "Transform coefficient histogram-based image enhancement algorithms using contrast entropy," *IEEE Trans. Image Process.*, vol. 16, no. 3, pp. 741–758, Mar. 2007.
[36] N. Petrick, H.-P. Chan, B. Sahiner, and D. Wei, "An adaptive density-weighted contrast enhancement filter for mammographic breast mass detection," *IEEE Trans. Med. Imag.*, vol. 15, no. 1, pp. 59–67, Feb. 1996.
[37] W. Qian, L. P. Clarke, M. Kallergi, and R. A. Clark, "Tree-structured nonlinear filters in digital mammography," *IEEE Trans. Med. Imag.*, vol. 13, no. 1, pp. 25–36, Mar. 1994.
[38] Y. Zhou, K. Panetta, and S. Agaian, "Human visual system based mammogram enhancement and analysis," in *Proc. 2010 IEEE Int. Conf. Image Process. Theory Tools Appl.*, Paris, France, pp. 229–234.
[39] A. P. Dhawan, G. Buelloni, and R. Gordon, "Enhancement of mammographic features by optimal adaptive neighborhood image processing," *IEEE Trans. Med. Imag.*, vol. MI-5, no. 1, pp. 8–15, Mar. 1986.
[40] V. H. Guis, M. Adel, M. Rasigni, G. Rasigni, B. Seradour, and P. Heid, "Adaptive neighborhood contrast enhancement in mammographic phantom images," *Opt. Eng.*, vol. 42, pp. 357–366, 2003.
[41] G. Ramponi, N. K. Strobel, S. K. Mitra, and T.-H. Yu, "Nonlinear unsharp masking methods for image contrast enhancement," *J. Electron. Imag.*, vol. 5, pp. 353–366, 1996.
[42] Z. Wu, J. Yuan, B. Lv, and X. Zheng, "Digital mammography image enhancement using improved unsharp masking approach," in *Proc. 2010 3rd Int. Congr. Image Signal Process.*, pp. 668–672.
[43] J. George and S. P. Indu, "Fast adaptive anisotropic filtering for medical image enhancement," in *Proc. 2008 IEEE Int. Symp. Signal Process. Inf. Technol.*, pp. 227–232.
[44] A. Polesel, G. Ramponi, and V. J. Mathews, "Image enhancement via adaptive unsharp masking," *IEEE Trans. Image Process.*, vol. 9, no. 3, pp. 505–510, Mar. 2000.
[45] G. Ramponi and A. Polesel, "Rational unsharp masking technique," *J. Electron. Imag.*, vol. 7, pp. 333–338, 1998.
[46] N. Strobel and S. K. Mitra, "Quadratic filters for image contrast enhancement," in *Proc. 1994 28th Asilomar Conf. Signals, Syst. Comput.*, vol. 1, pp. 208–212.
[47] G. Ramponi, "A cubic unsharp masking technique for contrast enhancement," *Signal Process.*, vol. 67, pp. 211–222, 1998.
[48] S. Singh and K. Bovis, "An evaluation of contrast enhancement techniques for mammographic breast masses," *IEEE Trans. Inf. Technol. Biomed.*, vol. 9, no. 1, pp. 109–119, Mar. 2005.
[49] S. M. Pizer, E. P. Amburn, J. D. Austin, R. Cromartie, A. Geselowitz, T. Greer, B. ter Haar Romeny, J. B. Zimmerman, and K. Zuiderveld, "Adaptive histogram equalization and its variations," *Comput. Vis. Graph.*, vol. 39, pp. 355–368, 1987.
[50] K. Panetta, S. Agaian, Y. Zhou, and E. J. Wharton, "Parameterized logarithmic framework for image enhancement," *IEEE Trans. Syst., Man, Cybern. B, Cybern.*, vol. 41, no. 2, pp. 460–473, Apr. 2011.
[51] M. Jourlin and J. Pinoli, "A model for logarithmic image processing," *J. Microsc.*, vol. 149, pp. 21–35, 1988.
[52] K. A. Panetta, E. J. Wharton, and S. S. Agaian, "Human visual system-based image enhancement and logarithmic contrast measure," *IEEE Trans. Syst., Man, Cybern. B, Cybern.*, vol. 38, no. 1, pp. 174–188, Feb. 2008.
[53] S. DelMarco and S. Agaian, "The design of wavelets for image enhancement and target detection," in *Proc. Mobile Multimedia/Image Process., Security, Appl.*, Orlando, FL, 2009, pp. 735103-1–735103-12.
[54] ITU-T, "Methods for subjective determination of transmission quality," Recommendation: International Telecommunication Union, Geneva, Switzerland, P. 800, 1996.
[55] J. Suckling, J. Parker, D. Dance, S. Astley, I. Hutt, C. Boggis, I. Ricketts, E. Stamatakis, N. Cerneaz, and S. Kok, "The mammographic image analysis society digital mammogram database," in *Proc. 2nd Int. Workshop Digital Mammography*, 1994, pp. 375–378.
[56] M. K. Kundu and S. K. Pal, "Thresholding for edge detection using human psychovisual phenomena," *Pattern Recognit. Lett.*, vol. 4, pp. 433–441, 1986.
[57] G. Buchsbaum, "An analytical derivation of visual nonlinearity," *IEEE Trans. Biomed. Eng.*, vol. BME-27, no. 5, pp. 237–242, May 1980.
[58] M. J. P. Castanho, L. C. Barros, A. Yamakami, and L. L. Vendite, "Fuzzy receiver operating characteristic curve: An option to evaluate diagnostic tests," *IEEE Trans. Inf. Technol. Biomed.*, vol. 11, no. 3, pp. 244–250, May 2007.
[59] M. Zweig and G. Campbell, "Receiver-operating characteristic (ROC) plots: A fundamental evaluation tool in clinical medicine," *Clin. Chem.*, vol. 39, pp. 561–577, Apr. 1993.
[60] Wikipedia. (2011, May 11). Receiver operating characteristic. [Online]. Available: http://en.wikipedia.org/wiki/Receiver_operating_characteristic.
[61] A. Slaby, "ROC analysis with Matlab," in *Proc. 2007 29th Int. Conf. Inf. Technol. Interfaces*, Cavtat, Croatia, pp. 191–196.
[62] J. Eng. (2007, Sep. 17). ROC analysis: Web-based calculator for ROC curves. [Online]. Available: http://www.jrocfit.org.

Karen Panetta (S'84–M'85–SM'95–F'08) received the B.S. degree in computer engineering from Boston University, Boston, MA, and the M.S. and Ph.D. degrees in electrical engineering from Northeastern University, Boston.

She is currently a Professor of electrical and computer engineering at Tufts University, Medford, MA, and the Founder of the Nerd Girls Program to promote women in engineering. She is also a Consulting Engineer with Tyco Electronics, Inc., Lowell, MA. She is a cofounder of BA Logix, Inc., Quincy, MA, and serves as the company's Chief Research Scientist. She was the 2007–2009 IEEE Director of Women in Engineering and the Editor-in-Chief of the IEEE WOMEN IN ENGINEERING MAGAZINE.

Yicong Zhou (M'07) received the B.S. degree in electrical engineering from Hunan University, Changsha, China, and the M.S. and Ph.D. degrees in electrical engineering from Tufts University, Medford, MA.

He is currently an Assistant Professor in the Department of Computer and Information Science, University of Macau, Macau, China. His current research interests include multimedia security, image enhancement, medical imaging, and signal/image processing.

Dr. Zhou is a member of the International Society for Optical Engineers (SPIE).

Sos Agaian (M'98–SM'00) received the M.S. degree (*summa cum laude*) in mathematics and mechanics from Yerevan State University, Yerevan, Armenia, the Ph.D. degree in mathematics and physics and the Doctor of Engineering Sciences (equivalent to the U.S. Doctor of Electrical and Computer Engineering) degree from the Academy of Sciences of the USSR, Moscow, Russia, and the Diploma in computer science (equivalent to the U.S. Ph.D. degree in computer science) from the Supreme Attestation Board of the USSR, Moscow.

He is currently the Peter T. Flawn Distinguished Professor in the College of Engineering, The University of Texas at San Antonio, San Antonio, and an Adjunct Professor in the Department of Electrical and Computer Engineering, Tufts University, Medford, MA. He is an Associate Editor of the *Journal of Real-Time Imaging* and the *Journal of Electronic Imaging, and an* editorial board member of the *Journal of Pattern Recognition and Image Analysis*. He has authored or coauthored more than 370 scientific papers, four books, and holds 13 patents. His current research interests include the broad area of signal/image processing and transmission, information security, and mobile imaging and secure communication.

Dr. Agaian is a Fellow of the International Society for Photo-Optical Instrumentations Engineers (SPIE).

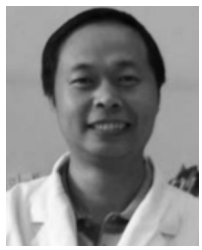

Hongwei Jia received the B.M. degree in clinical medicine from Xinxiang Medical School, Henan, China.

He is currently a Surgeon in the First People's Hospital of Pingdingshan, Henan. His current research interests include breast cancer, liver, and thyroid surgery.